Supplementary Information to

Reaching with the sixth sense: vestibular contributions to voluntary motor control in the human right parietal cortex

Alexandra Reichenbach, Jean-Pierre Bresciani, Heinrich H. Bülthoff, Axel Thielscher

S1. Supplementary Material and Methods

S1.1. Technical Setup

The experiment took place in the 12x12m Cyberneum Tracking Lab (MPI Tübingen;

http://www.cyberneum.de/research-facilities/trackinglab.html), in which the position of infrared-

reflective rigid-body marker objects can be identified in 3D using an optical tracking system of

16 infrared Vicon MX13 cameras (Vicon Motion Systems, Oxford, UK). Tracking and recording

of objects was accomplished using ViconTracker software with a sampling rate of 120Hz.

Participants sat comfortably in a robotic wheelchair capable of 360° rotations (BlueBotics,

Lausanne, Switzerland; http://www.cyberneum.de/de/technische-ausstattung/treadmills-

more.html). The position and orientation of the participants' right hand and the wheelchair was

tracked using four Vicon markers each (Schomaker et al., 2011). A black table was mounted

above the participants lap (Fig. 1), on which a keypad was fixated in the bottom left corner (hand

starting position), and a white LED on the middle top (body-fixed visual fixation). Additionally,

an earth-fixed red laser pointer from above indicated the target position on the table in the top

right corner. The distance of the target with respect to the starting position was adjusted for each

subject individually to accommodate for different arm lengths. For fixating the participants'

body and head with respect to the wheelchair and stably attaching the TMS coil, a custom-built

black aluminium frame was mounted on the chair. A chin and forehead rest fixated the head

above the rotation axis with the head tilted downward to allow direct line of sight on the fixation

LED and the target. The TMS coil was attached on the frame at one side of the head. Control

over the experiment and data recording was accomplished using custom-written MATLAB

routines (The MathWorks, Natick, MA, USA) incorporating Cogent 2000 (University College

London, London, UK).

S1.2. Trial Timing and Rotation Profile
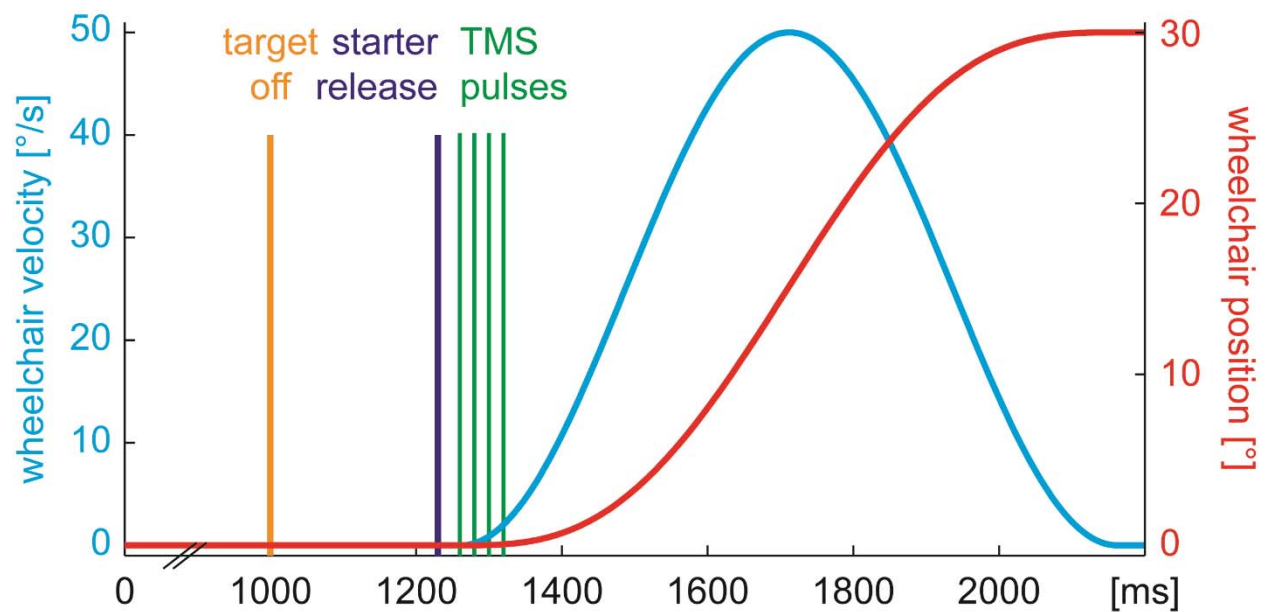
Figure S1   Schematics of the timing of one trial, aligned to the initiation of the trial (start button press, which triggered switching on the fixation and target LEDs). Velocity and position of the wheelchair is exemplary depicted for a +30° rotation.

S1.3. TMS Stimulation Sites

All TMS sites were chosen because processing of vestibular information or sensory processing for online motor control during reaching has been reported on either the site itself or the mirror-symmetric site on the other hemisphere. Furthermore, we tried to cover a large area over the PPC with roughly equidistantly distributed stimulation sites, mirrored across hemispheres.

The MNI coordinates of the grid were transformed from MNI space (Mazziotta et al., 2001) to the space of the individual structural images using the linear registration (FLIRT) of FSL 4.0 (FMRIB, Oxford, UK; (Smith et al., 2005; Smith et al., 2004). The closest coil position on the skull of every participant was determined for each coil position using custom-written MATLAB routines and the surface reconstruction of the skull as obtained with BrainVoyager 2000 (Brain Innovation, Maastricht, The Netherlands).

- Left (right) IPS1 (MNI (x/y/z) [mm]: -(+)44/-42/55), anatomical: anterior IPS

  Reason for inclusion in the study: TMS studies on visual (Reichenbach et al., 2011) and multi-sensory (Reichenbach et al., 2014) processing have identified the left aIPS as a key region for sensory processing during online motor control.

- Left (right) IPS2 (MNI (x/y/z) [mm]: -(+)30/-30/50), anatomical: anterior part of medial IPS[1]

  Reason for inclusion in the study: consistent bilateral fMRI activation during galvanic vestibular stimulation (Stephan et al., 2005). The coordinates are based on the cluster peak in the left hemisphere but the cluster peak in the right hemisphere is located within 5mm distance as well.

---

[1] The medial IPS (mIPS) has been suggested as the human homologue to the parietal reach region (PRR) Grefkes, C., Fink, G.R., 2005. The functional organization of the intraparietal sulcus in humans and monkeys. J Anat 207, 3-17.

- Left (right) IPS3 (MNI (x/y/z) [mm]: -(+)36/-64/54), anatomical: posterior part of mIPS[1]

  Reason for inclusion in the study: TMS studies have identified the left posterior mIPS as a key region for proprioceptive processing for motor control (Chib et al., 2009; Della-Maggiore et al., 2004; Reichenbach et al., 2014). Additionally, fMRI activation in the left and right posterior mIPS during caloric vestibular stimulation peaked within less than 10mm of the stimulation site (Suzuki et al., 2001).

- Left (right) IPS4 (MNI (x/y/z) [mm]: -(+)40/-76/47), anatomical: caudal IPS, angular gyrus

  Reason for inclusion in the study: TMS over P3/P4[2] disrupted path integration during a vestibular navigation task (Seemungal et al., 2008).

- Left (right) TPJ (MNI (x/y/z) [mm]: -(+)72/-38/36), anatomical: temporo-parietal junction

  Reason for inclusion in the study: consistent (bilateral) fMRI activation during caloric vestibular stimulation (Dieterich et al., 2003). The coordinates are based on the cluster peak in the left hemisphere but the cluster peak in the right hemisphere is located within 9mm distance as well.

---

[2] P3/P4 corresponds to our stimulation sites IPS4 according to Okamoto, M., Dan, H., Sakamoto, K., Takeo, K., Shimizu, K., Kohno, S., Oda, I., Isobe, S., Suzuki, T., Kohyama, K., Dan, I., 2004. Three-dimensional probabilistic anatomical cranio-cerebral correlation via the international 10-20 system oriented for transcranial functional brain mapping. Neuroimage 21, 99-111.
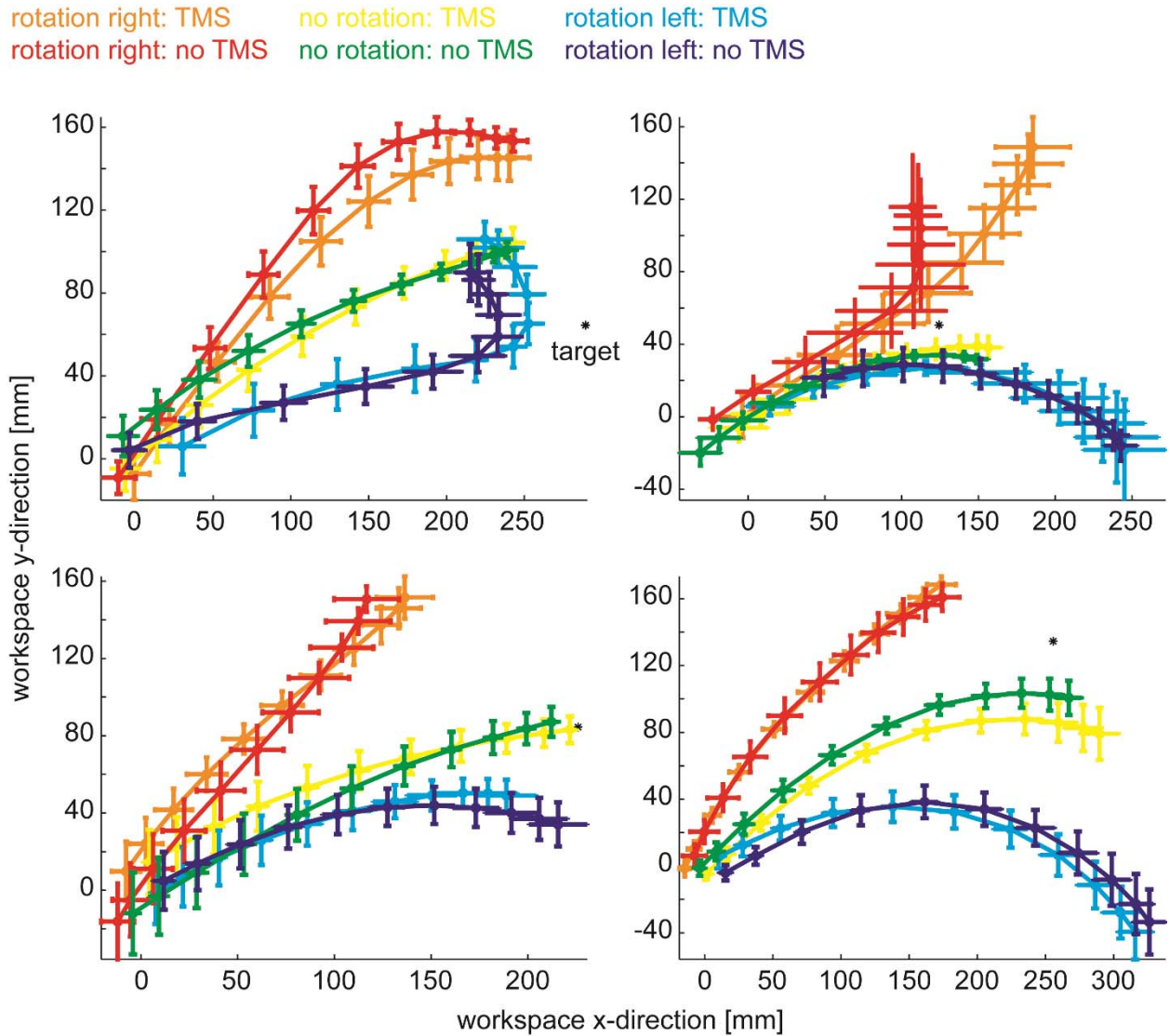
S2. Supplementary Data

S2.1. Reaching Behavior Averaged Across TMS Stimulation Sites

Mean summary statistics averaged across all stimulation sites (mean (SEM)).

		EndAng [°]	EndDevX	EndDevY	EndVarX	EndVarY	MT [ms]
no rotation	TMS	4.0 (2.6)	6.7 (4.5)	98.6 (3.0)	10.7 (0.8)	9.0 (0.8)	945 (47)
	no TMS	3.7 (2.7)	6.2 (4.6)	97.7 (2.7)	10.4(0.9)	10.3 (1.4)	960 (41)
	TMS effect	$t_9 = 1.53$	$t_9 = 1.38$	$t_9 = 1.84$	$t_9 = 1.01$	$t_9 = 1.24$	$t_9 = 1.12$
		$p = .161$	$p = .202$	$p = .098$	$p = .337$	$p = .247$	$p = .292$
rotation left	TMS	16.8 (3.9)	30.4 (7.2)	96.3 (3.6)	19.5 (1.8)	15.2 (1.7)	993 (38)
	no TMS	16.7 (3.9)	29.7 (7.1)	95.5 (3.3)	19.8 (2.4)	15.2 (1.6)	1013 (38)
	TMS effect	$t_9 = 0.21$	$t_9 = 0.60$	$t_9 = 1.19$	$t_9 = 0.24$	$t_9 = 0.02$	$t_9 = 1.63$
		$p = .837$	$p = .565$	$p = .265$	$p = .816$	$p = .986$	$p = .137$
rotation right	TMS	-11.8 (3.5)	-20.6 (6.8)	99.2 (5.2)	19.9 (3.3)	17.6 (3.1)	1071 (50)
	no TMS	-12.1 (3.9)	-21.0 (7.6)	98.6 (5.8)	18.8 (3.0)	15.6 (1.7)	1065 (47)
	TMS effect	$t_9 = 0.36$	$t_9 = 0.29$	$t_9 = 0.64$	$t_9 = 1.06$	$t_9 = 0.99$	$t_9 = 0.66$
		$p = .731$	$p = .782$	$p = .541$	$p = .318$	$p = .348$	$p = .528$

S2.2. Exemplary Non-normalized Single Subject Trajectories

rotation right: TMS   no rotation: TMS   rotation left: TMS
rotation right: no TMS   no rotation: no TMS   rotation left: no TMS

Figure S2   Non-normalized trajectory data for a single experimental block for 4 exemplary participants for TMS stimulation site right IPS3 in world coordinates relative to movement start. The error bars denote ± 1 SEM.

S2.3. Average Group Trajectories for All Stimulation Sites
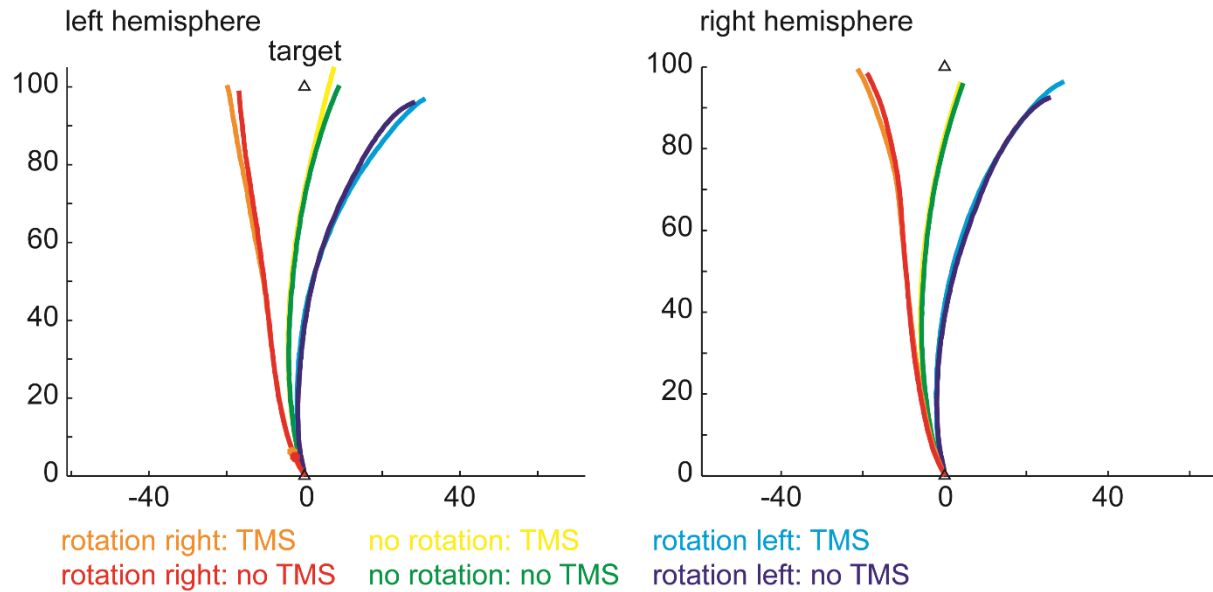
Figure S3   Average group trajectories for the TMS stimulation sites IPS1. The axes are arbitrary units, spatially normalized to the individual target positions at 0/100. The stars / bold parts indicate the positions where the x directions differed significantly between TMS and no TMS trials across participants ($p < .05$, uncorrected).
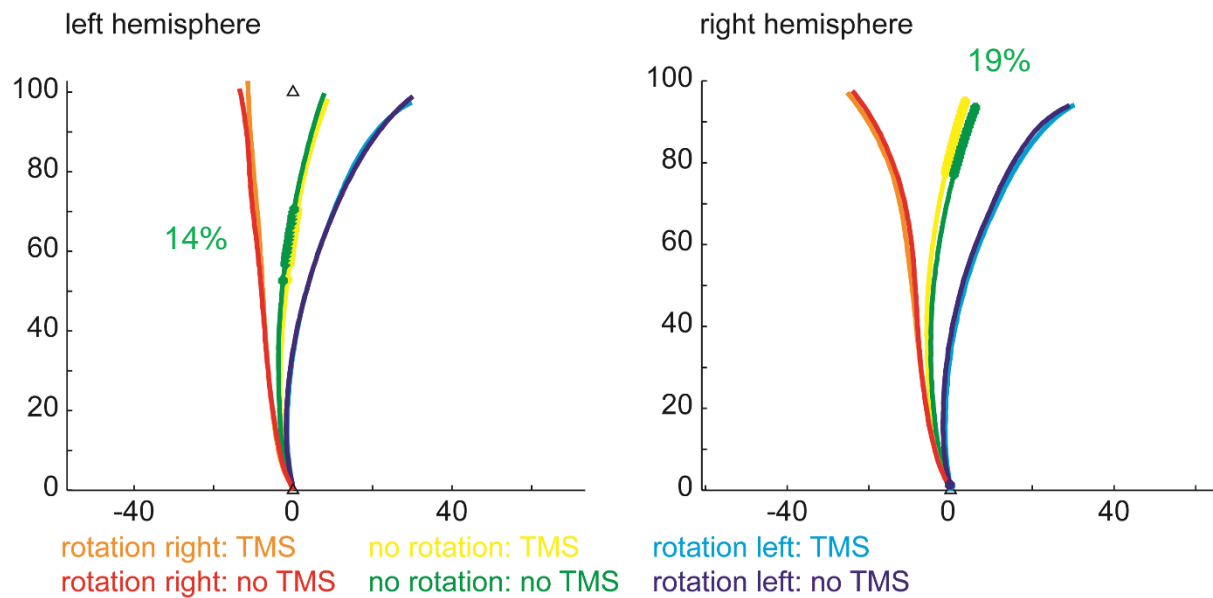
Figure S4   Average group trajectories for the TMS stimulation sites IPS2. Conventions analogue to Fig. S3. Note that the percentage indicates the proportion of **successive** significant tests.
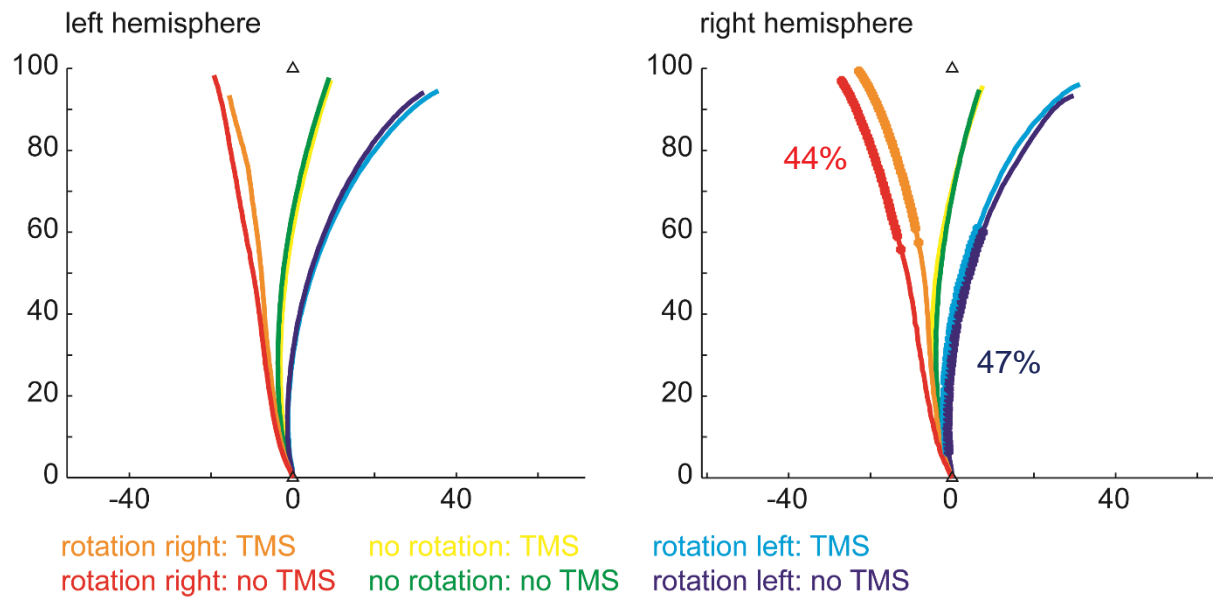
Figure S5   Average group trajectories for the TMS stimulation sites IPS3. Conventions analogue to Fig. S3. Note that the percentage indicates the proportion of **successive** significant tests.
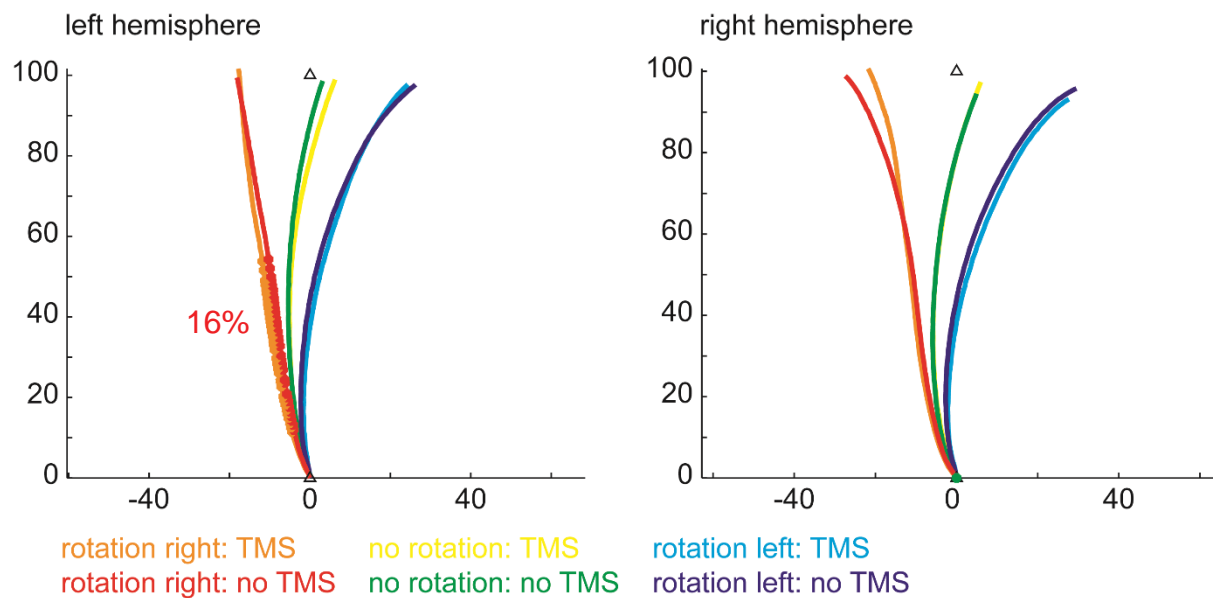
Figure S6   Average group trajectories for the TMS stimulation sites IPS4. Conventions analogue to Fig. S3. Note that the percentage indicates the proportion of **successive** significant tests.

left hemisphere   right hemisphere

rotation right: TMS   no rotation: TMS   rotation left: TMS
rotation right: no TMS   no rotation: no TMS   rotation left: no TMS

Figure S7   Average group trajectories for the TMS stimulation sites TPJ. Conventions analogue to Fig. S3. Note that the percentage indicates the proportion of **successive** significant tests.
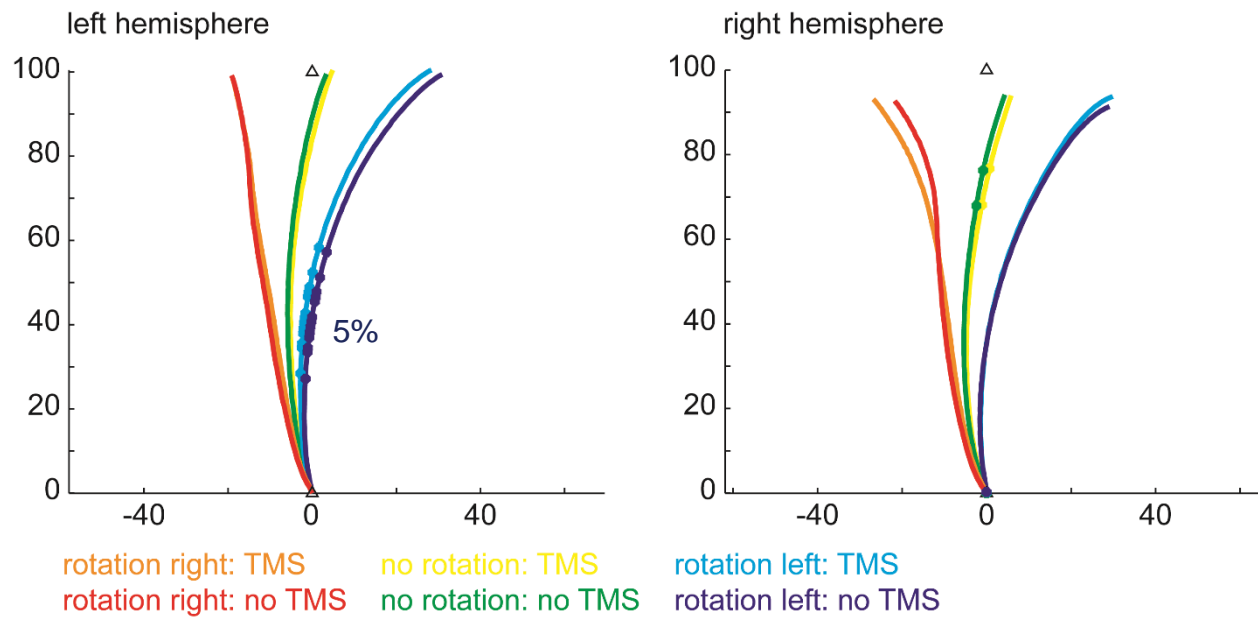
S2.4 Main statistics without participating author

Comparison of the main TMS effects reported in 3.2 without the participating author.

	N = 10	N = 9
EndDevX over right IPS3 (rotation right)		
mean (SEM)	-23.2 (6.6) / -27.2 (6.4)	-22.0 (7.0) / -26.3 (7.3)
t-test	$t_9 = 4.535; p = .001$	$t_8 = 4.564; p = .002$
EndAng over right IPS3 (rotation right)		
mean (SEM)	-13.3 (3.1) / -16.2 (3.3)	-12.4 (3.3) / -15.6 (3.7)
t-test	$t_9 = 3.741; p = .005$	$t_8 = 4.098; p = .003$
EndDevX right IPS3 > all other sites	$t_9 = 2.501; p = .017$	$t_8 = 2.368; p = .023$

S2.5 Further exploratory analyses

In order to test whether the TMS effect we found might be mediated by differences in setup or motor behavior between subjects, we conducted some additional analyses on the condition with the robust TMS effect, the impairment of *EndDevX* during the rightward rotation when stimulating rIPS3. Specifically, we looked for a relationship between the visual angle of the target and the TMS effect on *EndDevX* but found no strong between-subject correlation ($R^2 = 0.150; p = .269$). The same negative result was obtained for the correlation between visual angle and effect on *EndVarX* ($R^2 = 0.089; p = .403$). Furthermore, neither the maximum reaching velocity ($R^2 < 0.001; p = .955$) nor total movement time ($R^2 = 0.012; p = .764$) revealed a relationship between the strength of the TMS effect and those kinematic measures.

Given that we do not find a relationship of these factors with the TMS effect in the condition with the strongest effect, it seems unlikely that any other site or dependent measure would be related with them.

S2.6 Detailed data and statistics

Mean summary statistics for the detailed conditions (mean (SEM)). Significant changes resulting from TMS stimulation are marked bold (uncorrected $\alpha = .05$) and red (Bonferroni corrected $\alpha = .005$).

		EndAng [°]	EndDevX	EndDevY	EndVarX	EndVarY	MT [ms]
left IPS1							
no rotation	TMS	4.5 (2.8)	7.9 (5.1)	105.9 (3.4)	11.3 (0.9)	9.6 (1.5)	985 (83)
	no TMS	5.4 (3.2)	9.3 (5.8)	101. (2.9)	12.1 (1.2)	8.7 (1.8)	975 (54)
	TMS effect	$p = .404$	$p = .412$	$p = .054$	$p = .641$	$p = .326$	$p = .862$
rotation left	TMS	17.5 (4.0)	31.7 (7.8)	97.3 (4.3)	20.8 (1.8)	15.8 (2.5)	1009 (44)
	no TMS	16.0 (4.9)	29.0 (9.2)	96.3 (3.7)	23.3 (3.6)	18.4 (4.0)	1038 (51)
	TMS effect	$p = .396$	$p = .465$	$p = .660$	$p = .469$	$p = .615$	$p = .258$
rotation right	TMS	-10.2 (5.4)	-20 (11.5)	10.9 (2.9)	20.8 (3.9)	14.4 (1.4)	1103 (60)
	no TMS	-10.1 (5.5)	-17.0 (10.1)	99.7 (4.4)	19.3 (5.3)	15.8 (2.2)	1109 (4)
	TMS effect	$p = .930$	$p = .410$	$p = .323$	$p = .614$	$p = .323$	$p = .894$
left IPS2							
no rotation	TMS	5.4 (2.4)	9.0 (4.0)	99.1 (3.6)	10.7 (2.3)	9.6 (2.1)	971 (54)
	no TMS	4.7 (2.5)	8.2 (4.4)	100.6 (3.8)	9.2 (1.1)	8.1 (0.7)	1025 (55)
	TMS effect	$p = .229$	$p = .476$	$p = .360$	$p = .438$	$p = .362$	$p = .330$
rotation left	TMS	16.9 (3.8)	30.4 (6.8)	97.5 (4.2)	20.4 (3.5)	14.6 (2.5)	1007 (33)
	no TMS	16.9 (3.5)	30.7 (6.8)	99.2 (4.6)	19.5 (3.5)	13.3 (2.0)	1022 (46)
	TMS effect	$p = .981$	$p = .903$	$p = .330$	$p = .729$	$p = .434$	$p = .756$
rotation right	TMS	-6.5 (4.9)	-11.7 (9.5)	103.7 (5.2)	18.6 (3.6)	18.6 (3.4)	1089 (59)
	no TMS	-7.4 (5.4)	-13.7 (11.3)	101.4 (5.3)	18.3 (3.5)	16.7 (1.8)	1086 (64)
	TMS effect	$p = .424$	$p = .460$	$p = .240$	$p = .913$	$p = .401$	$p = .926$
left IPS3							
no rotation	TMS	5.8 (2.9)	9.6 (4.8)	98.0 (4.1)	11.1 (1.5)	8.8 (0.8)	919 (48)
	no TMS	5.6 (3.0)	9.1 (5.1)	98.6 (3.7)	10.6 (1.4)	8.9 (1.3)	954 (56)
	TMS effect	$p = .803$	$p = .736$	$p = .597$	$p = .729$	$p = .967$	$p = .286$
rotation left	TMS	20.6 (4.1)	36.2 (7.1)	94.7 (4.6)	22.4 (2.0)	17.7 (2.5)	1001 (48)
	no TMS	19.0 (4.1)	32.6 (7.0)	94.4 (4.8)	21.3 (2.3)	15.3 (2.0)	1026 (49)
	TMS effect	$p = .328$	$p = .240$	$p = .913$	$p = .451$	$p = .110$	$p = .577$
rotation right	TMS	-9.6 (5.0)	-15.8 (8.7)	93.9 (4.4)	22.8 (4.8)	18.6 (5.1)	1004 (62)
	no TMS	-10.1 (5.3)	-19.6 (10.8)	98.9 (5.6)	19.4 (3.7)	17.2 (2.9)	1023 (53)
	TMS effect	$p = .753$	$p = .343$	$p = .115$	$p = .219$	$p = .612$	$p = .676$
left IPS4							
no rotation	TMS	3.9 (2.7)	6.6 (4.6)	99.7 (3.3)	10.5 (1.1)	10.2 (1.5)	931 (55)
	no TMS	2.2 (3.0)	3.4 (5.1)	99.3 (3.8)	12.3 (1.4)	12.0 (1.9)	930 (46)
	TMS effect	$p = .087$	$p = .051$	$p = .735$	***p = .030***	$p = .105$	$p = .971$
rotation left	TMS	14.0 (3.2)	24.8 (6.2)	98.1 (3.9)	22.5 (2.7)	16.8 (2.2)	953 (58)
	no TMS	14.8 (3.8)	26.8 (6.9)	98.0 (4.7)	16.3 (1.4)	15.5 (2.8)	962 (43)
	TMS effect	$p = .546$	$p = .441$	$p = .971$	***p = .011***	$p = .518$	$p = .841$
rotation right	TMS	-10.0 (4.7)	-18.0 (9.0)	102.4 (5.4)	18.6 (3.5)	22.1 (4.4)	1002 (38)
	no TMS	-9.9 (5.1)	-18.4 (10.2)	100.0 (5.3)	18.1 (3.3)	17.0 (3.3)	953 (66)
	TMS effect	$p = .944$	$p = .617$	$p = .517$	$p = .617$	***p = .034***	$p = .249$
left TPJ							
no rotation	TMS	3.1 (2.6)	5.2 (4.7)	101.2 (2.7)	11.8 (1.0)	8.3 (1.0)	938 (19)
	no TMS	2.2 (2.5)	3.7 (4.5)	100.3 (2.8)	11.1 (1.5)	8.8 (1.4)	937 (23)
	TMS effect	$p = .224$	$p = .238$	$p = .127$	$p = .568$	$p = .598$	$p = .952$
rotation left	TMS	15.6 (3.5)	29.9 (8.7)	100.8 (3.7)	17.5 (1.7)	13.7 (2.2)	974 (36)
	no TMS	17.4 (3.0)	26.9 (8.3)	99.6 (4.3)	18.0 (1.8)	13.0 (2.4)	1037 (51)
	TMS effect	$p = .147$	$p = .243$	$p = .558$	$p = .810$	$p = .611$	$p = .070$
rotation right	TMS	-11.2 (4.5)	-19.1 (8.6)	99.0 (4.6)	20.9 (5.0)	18.1 (5.1)	1072 (46)
	no TMS	-10.7 (3.9)	-19.4 (8.0)	99.8 (3.5)	21.3 (4.5)	15.1 (1.5)	1025 (39)
	TMS effect	$p = .716$	$p = .884$	$p = .722$	$p = .891$	$p = .533$	$p = .204$

		EndAng [°]	EndDevX	EndDevY	EndVarX	EndVarY	MT [ms]
right IPS1							
no rotation	TMS	2.8 (3.5)	4.2 (5.9)	97.1 (3.3)	9.2 (1.7)	7.9 (0.8)	978 (34)
	no TMS	3.1 (3.4)	4.8 (5.7)	96.8 (3.1)	8.4 (1.3)	12.0 (3.5)	965 (37)
	TMS effect	*p* = .773	*p* = .678	*p* = .848	*p* = .475	*p* = .236	*p* = .666
rotation left	TMS	16.5 (4.8)	29.9 (8.7)	96.6 (4.2)	17.9 (2.1)	13.4 (2.0)	1034 (38)
	no TMS	15.8 (4.9)	26.9 (8.3)	92.5 (3.9)	19.8 (3.3)	15.3 (2.5)	988 (36)
	TMS effect	*p* = .557	*p* = .370	***p = .045***	*p* = .551	*p* = .222	*p* = .269
rotation right	TMS	-12.6 (2.9)	-21.8 (5.1)	100.0 (3.6)	18.1 (2.7)	18.1 (3.9)	1085 (53)
	no TMS	-11.9 (3.6)	-19.5 (5.9)	99.1 (7.3)	19.0 (2.6)	15.5 (2.1)	1078 (36)
	TMS effect	*p* = .741	*p* = .481	*p* = .627	*p* = .538	*p* = .456	*p* = .806
right IPS2							
no rotation	TMS	2.4 (3.5)	3.9 (6.0)	95.8 (3.0)	10.6 (1.2)	9.9 (2.5)	923 (72)
	no TMS	3.9 (3.9)	6.4 (6.6)	94.2 (2.5)	10.4 (1.0)	12.4 (2.6)	957 (43)
	TMS effect	***p = .026***	***p = .027***	*p* = .300	*p* = .833	*p* = .531	*p* = .494
rotation left	TMS	16.7 (5.7)	30.9 (10.4)	94.4 (3.4)	18.6 (3.0)	16.4 (3.1)	931 (96)
	no TMS	16.6 (5.2)	29.6 (9.0)	94.1 (3.8)	19.7 (3.3)	15.3 (2.1)	1002 (56)
	TMS effect	*p* = .942	*p* = .694	*p* = .883	*p* = .983	*p* = .458	*p* = .184
rotation right	TMS	-14.8 (3.3)	-25.9 (6.0)	97.5 (7.6)	18.3 (4.2)	14.3 (3.8)	1096 (62)
	no TMS	-15.0 (3.9)	-24.5 (6.4)	98.0 (8.2)	15.7 (1.9)	13.2 (1.8)	1101 (72)
	TMS effect	*p* = .889	*p* = .537	*p* = .779	*p* = .537	*p* = .731	*p* = .888
right IPS3							
no rotation	TMS	4.8 (3.8)	7.8 (6.3)	96.6 (3.6)	10.2 (1.7)	7.1 (1.1)	907 (89)
	no TMS	4.2 (3.6)	6.9 (6.0)	95.6 (2.8)	8.9 (1.4)	10.7 (2.4)	884 (89)
	TMS effect	*p* = .161	*p* = .258	*p* = .444	*p* = .280	*p* = .196	*p* = .365
rotation left	TMS	17.3 (5.6)	31.9 (9.6)	96.2 (6.0)	18.1 (2.5)	12.3 (2.5)	985 (86)
	no TMS	17.3 (5.3)	30.2 (8.9)	93.4 (4.5)	20.8 (5.1)	13.9 (2.5)	1007 (101)
	TMS effect	*p* = .990	*p* = .463	*p* = .263	*p* = .378	*p* = .401	*p* = .707
rotation right	TMS	-13.3 (3.1)	-23.2 (6.4)	99.9 (8.5)	17.3 (2.2)	16.3 (2.7)	1021 (104)
	no TMS	-16.2 (3.3)	-27.2 (6.6)	96.8 (8.4)	16.8 (3.4)	13.3 (1.8)	1031 (103)
	TMS effect	***p = .005***	***p = .001***	*p* = .216	*p* = .810	*p* = .312	*p* = .747
right IPS4							
no rotation	TMS	3.4 (3.1)	6.3 (5.7)	98.2 (3.2)	11.6 (1.8)	8.3 (1.0)	947 (69)
	no TMS	2.9 (3.3)	5.3 (5.7)	95.3 (3.0)	10.3 (1.4)	12.0 (3.4)	1010 (73)
	TMS effect	*p* = .488	*p* = .337	*p* = .100	*p* = .163	*p* = .327	*p* = .164
rotation left	TMS	15.6 (5.0)	28.2 (9.1)	93.3 (3.6)	20.0 (2.8)	13.7 (2.1)	1033 (51)
	no TMS	16.2 (5.0)	30.2 (9.5)	96.0 (4.3)	20.3 (3.3)	15.8 (2.1)	1033 (67)
	TMS effect	*p* = .532	*p* = .369	*p* = .222	*p* = .884	*p* = .326	*p* = .995
rotation right	TMS	-13.5 (3.0)	-23.0 (5.2)	101.5 (9.1)	21.7 (4.6)	17.1 (3.1)	1122 (95)
	no TMS	-16.2 (3.2)	-28.0 (6.2)	99.4 (9.5)	19.8 (4.3)	17.1 (2.7)	1112 (86)
	TMS effect	*p* = .175	*p* = .167	*p* = .359	*p* = .310	*p* = .996	*p* = .858
right TPJ							
no rotation	TMS	4.2 (3.3)	6.1 (5.1)	94.7 (4.1)	10.1 (1.1)	10.4 (2.3)	949 (46)
	no TMS	3.1 (3.2)	4.7 (5.0)	94.9 (3.8)	10.4 (2.0)	9.3 (2.0)	961 (49)
	TMS effect	*p* = .243	*p* = .190	*p* = .909	*p* = .817	*p* = .343	*p* = .654
rotation left	TMS	17.6 (5.2	30.5 (8.8)	93.9 (5.9)	16.8 (2.8)	17.2 (4.0)	1000 (35)
	no TMS	17.2 (5.4)	29.6 (9.0)	91.5 (4.8)	19.5 (3.5)	16.0 (2.4)	1015 (43)
	TMS effect	*p* = .790	*p* = .653	*p* = .211	*p* = .205	*p* = .647	*p* = .443
rotation right	TMS	-16.7 (3.8)	-27.3 (6.8)	93.5 (7.7)	21.4 (4.6)	18.3 (4.1)	1116 (61)
	no TMS	-13.4 (4.3)	-22.1 (7.4)	93.2 (6.8)	19.8 (2.3)	15.5 (2.1)	1130 (48)
	TMS effect	*p* = .123	*p* = .219	*p* = .814	*p* = .573	*p* = .297	*p* = .555

S2.7 Detailed analyses of across-trials variability

In order to test for TMS-induced increase in within-subject variability, we subjected the

trajectory data to two additional analyses. First, we calculated the average correlation between

the normalized x-positions for each subject and condition (see table below). This analysis did not

reveal any TMS effects on the variability. Second, we calculated the within-subject SEM for

each subject and condition and conducted an analysis analogue to the analysis of the mean

trajectories (cf. S2.3). Figure 8 demonstrates that TMS only influenced the variability of

rightward rotated trials when administered over the left TPJ. The effect however, a reduction in

variability, is inconsistent with the hypothesis of a disruption of information processing by TMS.

Mean correlation coefficient for the detailed conditions (mean (SEM)). Significant changes
resulting from TMS stimulation are marked bold (uncorrected α = .05).

	left hemisphere			*right hemisphere*		
	TMS	no TMS	TMS effect (p)	TMS	no TMS	TMS effect (p)
IPS1						
no rotation	0.44 (0.07)	0.42 (0.07)	.680	0.54 (0.07)	0.55 (0.08)	.909
rotation left	0.44 (0.08)	0.42 (0.09)	.584	0.43 (0.11)	0.36 (0.10)	.266
rotation right	0.49 (0.10)	0.49 (0.11)	.941	0.41 (0.10)	0.39 (0.10)	.831
IPS2						
no rotation	0.36 (0.08)	0.41 (0.09)	.482	0.41 (0.08)	0.42 (0.10)	.686
rotation left	0.50 (0.08)	0.51 (0.12)	.906	0.45 (0.10)	0.48 (0.10)	.594
rotation right	0.50 (0.11)	0.52 (0.12)	.585	0.42 (0.10)	0.48 (0.08)	.118
IPS3						
no rotation	0.44 (0.04)	0.47 (0.05)	.642	0.50 (0.10)	0.48 (0.10)	.558
rotation left	0.52 (0.07)	0.43 (0.10)	.252	0.56 (0.10)	0.44 (0.09)	.269
rotation right	0.45 (0.08)	0.51 (0.10)	.554	0.50 (0.11)	0.51 (0.10)	.480
IPS4						
no rotation	0.39 (0.09)	0.39 (0.09)	.891	0.43 (0.08)	0.45 (0.09)	.738
rotation left	0.31 (0.09)	0.43 (0.09)	**.028**	0.41 (0.10)	0.40 (0.11)	.647
rotation right	0.46 (0.10)	0.52 (0.12)	.485	0.44 (0.12)	0.54 (0.10)	.074
TPJ						
no rotation	0.33 (0.08)	0.30 (0.08)	.550	0.40 (0.11)	0.36 (0.10)	.271
rotation left	0.48 (0.08)	0.50 (0.08)	.615	0.42 (0.09)	0.35 (0.10)	.190
rotation right	0.44 (0.09)	0.43 (0.09)	.887	0.44 (0.09)	0.31 (0.12)	.154

left hemisphere   right hemisphere

rotation right: TMS   no rotation: TMS   rotation right: TMS
rotation right: no TMS   no rotation: no TMS   rotation right: no TMS
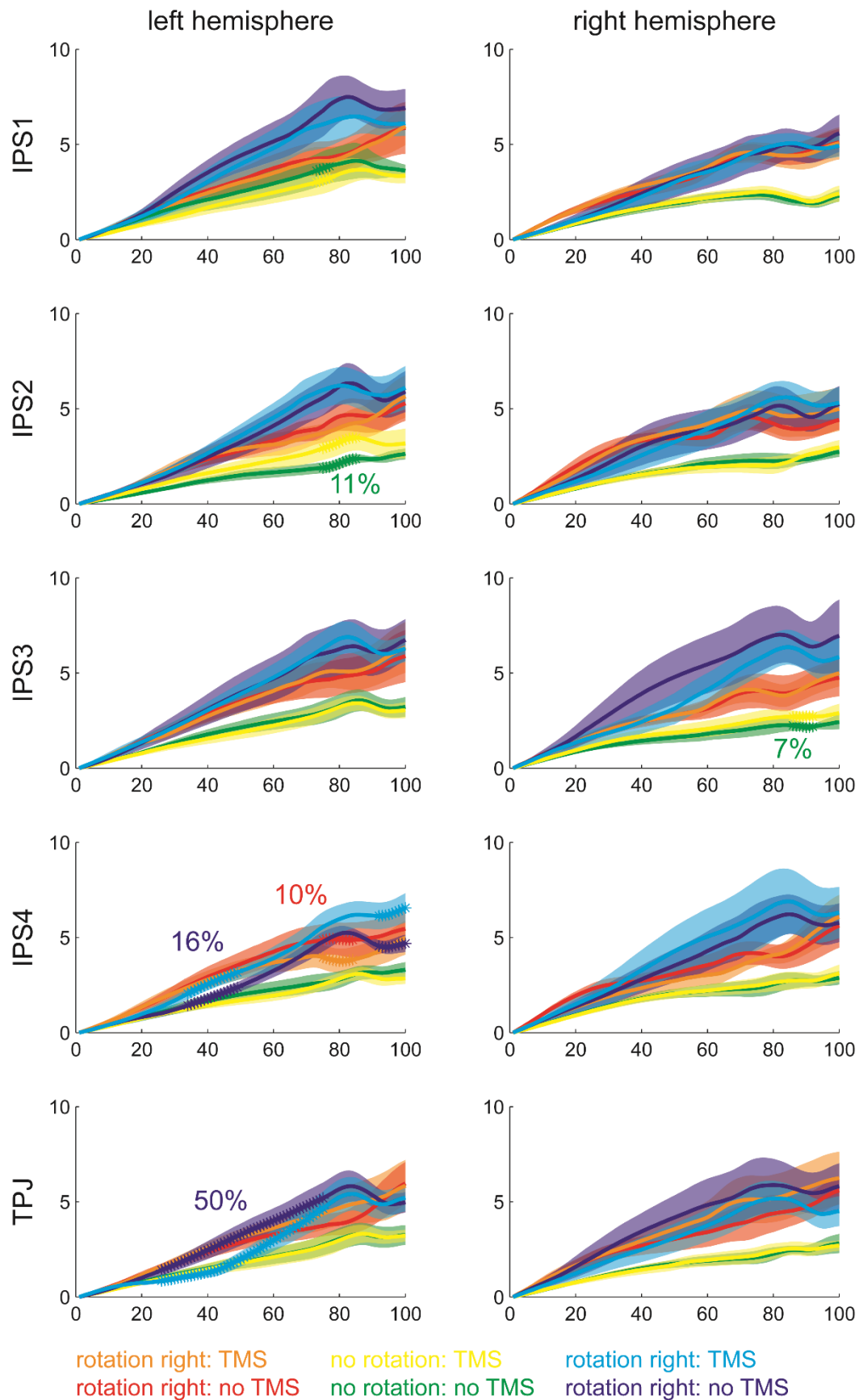
Figure S8   Average within-subject SEM in x direction along the trajectories. The x-axes denotes the 100 segments to which the data is normalized, and the y-axis the SEM in spatially normalized arbitrary units The stars / bold parts indicate the positions where the SEM differed significantly between TMS and no TMS trials across participants ($p < .05$, uncorrected). Note that the percentages indicate the proportion of **successive** significant tests.

S3. Supplementary References

Chib, V.S., Krutky, M.A., Lynch, K.M., Mussa-Ivaldi, F.A., 2009. The separate neural control of hand movements and contact forces. J Neurosci 29, 3939-3947.

Della-Maggiore, V., Malfait, N., Ostry, D.J., Paus, T., 2004. Stimulation of the posterior parietal cortex interferes with arm trajectory adjustments during the learning of new dynamics. J Neurosci 24, 9971-9976.

Dieterich, M., Bense, S., Lutz, S., Drzezga, A., Stephan, T., Bartenstein, P., Brandt, T., 2003. Dominance for vestibular cortical function in the non-dominant hemisphere. Cereb Cortex 13, 994-1007.

Grefkes, C., Fink, G.R., 2005. The functional organization of the intraparietal sulcus in humans and monkeys. J Anat 207, 3-17.

Mazziotta, J., Toga, A., Evans, A., Fox, P., Lancaster, J., Zilles, K., Woods, R., Paus, T., Simpson, G., Pike, B., Holmes, C., Collins, L., Thompson, P., MacDonald, D., Iacoboni, M., Schormann, T., Amunts, K., Palomero-Gallagher, N., Geyer, S., Parsons, L., Narr, K., Kabani, N., Le Goualher, G., Boomsma, D., Cannon, T., Kawashima, R., Mazoyer, B., 2001. A probabilistic atlas and reference system for the human brain: International Consortium for Brain Mapping (ICBM). Philos Trans R Soc Lond B Biol Sci 356, 1293-1322.

Okamoto, M., Dan, H., Sakamoto, K., Takeo, K., Shimizu, K., Kohno, S., Oda, I., Isobe, S., Suzuki, T., Kohyama, K., Dan, I., 2004. Three-dimensional probabilistic anatomical cranio-cerebral correlation via the international 10-20 system oriented for transcranial functional brain mapping. Neuroimage 21, 99-111.

Reichenbach, A., Bresciani, J.P., Peer, A., Bülthoff, H.H., Thielscher, A., 2011. Contributions of the PPC to online control of visually guided reaching movements assessed with fMRI-guided TMS. Cereb Cortex 21, 1602-1612.

Reichenbach, A., Thielscher, A., Peer, A., Bülthoff, H.H., Bresciani, J.P., 2014. A key region in the human parietal cortex for processing proprioceptive hand feedback during reaching movements. Neuroimage 84, 615-625.

Schomaker, J., Tesch, J., Bulthoff, H.H., Bresciani, J.P., 2011. It is all me: the effect of viewpoint on visual-vestibular recalibration. Exp Brain Res 213, 245-256.

Seemungal, B.M., Rizzo, V., Gresty, M.A., Rothwell, J.C., Bronstein, A.M., 2008. Posterior parietal rTMS disrupts human Path Integration during a vestibular navigation task. Neurosci Lett 437, 88-92.

Smith, S.M., Beckmann, C.F., Ramnani, N., Woolrich, M.W., Bannister, P.R., Jenkinson, M., Matthews, P.M., McGonigle, D.J., 2005. Variability in fMRI: a re-examination of inter-session differences. Hum Brain Mapp 24, 248-257.

Smith, S.M., Jenkinson, M., Woolrich, M.W., Beckmann, C.F., Behrens, T.E., Johansen-Berg, H., Bannister, P.R., De Luca, M., Drobnjak, I., Flitney, D.E., Niazy, R.K., Saunders, J., Vickers, J., Zhang, Y., De Stefano, N., Brady, J.M., Matthews, P.M., 2004. Advances in functional and structural MR image analysis and implementation as FSL. Neuroimage 23 Suppl 1, S208-219.

Stephan, T., Deutschlander, A., Nolte, A., Schneider, E., Wiesmann, M., Brandt, T., Dieterich, M., 2005. Functional MRI of galvanic vestibular stimulation with alternating currents at different frequencies. Neuroimage 26, 721-732.

Suzuki, M., Kitano, H., Ito, R., Kitanishi, T., Yazawa, Y., Ogawa, T., Shiino, A., Kitajima, K., 2001. Cortical and subcortical vestibular response to caloric stimulation detected by functional magnetic resonance imaging. Brain Res Cogn Brain Res 12, 441-449.